DEFENCE R&D DÉFENSE

A PDF-Module for Turbulent Deflagration Structure Computation

Fan Zhang
Defence Research Establishment Suffield
Box 4000, Stn Main
Medicine Hat, Alberta T1A 8K6

WARNING
"The use of this information is permitted subject to recognition of proprietary and patent rights."

DEFENCE RESEARCH ESTABLISHMENT SUFFIELD

Technical Report
DRES TR 1999-020

November 1999

National Defence / Défense nationale

Canada

A PDF-MODULE FOR TURBULENT DEFLAGRATION STRUCTURE COMPUTATION

DRES Technical Report TR 1999-020

Fan Zhang

Defence Research Establishment Suffield
Box 4000, Station Main, Medicine Hat, Alberta, Canada, T1A 8K6

October 1999

100-07192/

Abstract

In the FAE chemical initiation and the after-burning processes of oxygen-deficient explosives in various applications, a compressible, turbulent, fast flame with a "thick" distributed reaction zone is encountered. Owing to the complicated interaction between turbulent mixing and combustion, the physical mechanism for this fast turbulent flame regime leading to DDT has not been resolved and the numerical modelling is still in its pioneer stage.

This work was only a preliminary study in developing a model and its numerical scheme that describes a quasi-one-dimensional turbulent defraglation structure associated with local points on the flame front in the distributed flame regime. This quasi-one-dimensional model of turbulent flame structure can in future be coupled in a front-tracking algorithm that simulates the unsteady fast turbulent defraglation leading to a DDT process.

Owing to the stochastic nature and high turbulent intensity of the distributed flame regime, the model was based on Pope's PDF module and used a hybrid numerical scheme. In this scheme, the real chemical compositions and enthalpy were computed using the Monte Carlo method for the joint scalar PDF transport equations to capture the stochastic non-uniformity of the chemical compositions and temperature. The turbulent mean flow field was solved using a finite volume algorithm based on the method for pressure-implicit with splitting of operators to be compatible for a range of flow Mach numbers. The effect of the flame front curvature was modelled by source terms that are analogous to a quasi-1D area change term. The model was implemented in an unsteady version.

Acknowledgements

The author wishes to thank Professor Lie Zhao from the Institute of Mechanics, Chinese Academy of Sciences and Dr. Paul Thibault from Combustion Dynamics Ltd. for their contributions during the model development.

Table of Contents

Abstract ii

Acknowledgements iii

Table of contents iv

List of figures v

List of tables vii

1. Introduction 1

2. Monte Carlo method for scalar PDF transport equations 3

2.1. The joint scalar PAF equations for compressible flows 3

2.2. Monte Carlo method 6

3. PISO method for mean flow equations 9

3.1. The quasi-one-dimensional mean flow equations 9

3.2. Modified PISO method 12

3.2.1. Discretization 12

3.2.2. Splitting procedure 14

4. Coupling of Monte Carlo PDF and PISO mean flow scheme 15

5. An example: turbulent flame structure for a hydrogen-air mixture 17

6. Conclusions 22

References 23

List of Figures

Figure 1. The Borghi diagram 2

Figure 2. Schematic of the convection and diffusion transport of representative particles 7

Figure 3. Control volumes for velocity and scalar variables 13

Figure 4. Coupling of the Monte Carlo PDF and PISO mean flow scheme 16

Figure 5. Test case for quasi-1D turbulent flame structure 18

Figure 6. Mean flow velocity with and without curvature effects 19

Figure 7. Mean temperature with and without curvature effects 20

Figure 8. Turbulent kinetic energy with and without curvature effects 20

Figure 9. Turbulence dissipation rate with and without curvature effects 21

Figure 10. Mean mass fractions of H_2 and OH with and without curvature effects 21

Figure 11. Mean mass fractions of O_2 and H_2O with and without curvature effects 22

List of Tables

Table 1. Variables and functions in equations (3.13) 11

Table 2. Initial conditions for the test of turbulent premixed flame structure 19

A PDF-MODULE FOR TURBULENT DEFLAGRATION STRUCTURE COMPUTATION

Fan Zhang

Defence Research Establishment Suffield
Box 4000, Station Main, Medicine Hat, Alberta, Canada, T1A 8K6

1. Introduction

Conventional fuel-air explosives (FAE) have mostly used a direct detonation initiation with a strong external ignitor such as an exploding charge. This secondary ignition charge system increases the complexity and cost of the FAE systems. To simplify the design of FAE systems, the strong ignitor has been considered to be eliminated through the use of a catalyst or an elegant choice of a fuel mixture, which chemically triggers the fuel-air reaction so as to use the energy of the latter to promote detonation [1-2]. In this concept of chemical initiation, deflagration to detonation transition (DDT) is one of the great concerns, in which pre-shocked conditions established by the fuel dispersion and the production of radicals and hot spots are the keys leading to the onset of detonation. In certain cases, the early stage of DDT can be characterized by a fast flame that manifests itself through compressible, turbulent mixing of burned and unburned gases in the flame front. Such a compressible, turbulent combustion also plays an important role in the after-burning of detonation products in the air for oxygen-deficient high explosives [8]. Owing to the complicated interaction between turbulent mixing and combustion, the physical mechanism for the fast turbulent flame regime leading to DDT has not been resolved and the numerical modelling is still in its infant stage.

Turbulent combustion research has been greatly advanced through the recent works, in particular, by Bray, Moss, Libby, Peters, Pope and others [3-6]. We now have a better understanding of turbulent flame structure and their dependence on the chemical and turbulent time scales. Peters provided a systematical classification of various turbulent flame regimes using so-called Borghi diagram [4]. Figure 1 shows this diagram, in which the horizontal axis is the ratio of the turbulent integral scale versus laminar flame thickness and the vertical coordinate is the ratio of the turbulent velocity fluctuation versus the laminar flame speed. One important parameter in this diagram is the Karovitz number, $Ka = t_{ch} / t_K$, where t_{ch} is the chemical time scale and t_K is the micro-turbulent time scale associated with the small eddies at the Kolmogoroff dissipation scale. Another parameter is the Damköhler number, $Da = t_t / t_{ch}$, where t_t is the integral time scale of

turbulence. In the regime where Ka < 1, the turbulent flame can be viewed as a "brush" of laminar flames, and can be modelled using the flamelet models which have been developed extensively during the last two decades [6]. Outside of this regime, the intensity of turbulence is sufficiently large compared to the reaction rate, thus resulting in a "thick" distributed flame and local quenching. This is a regime where no a priori estimates for the flame structure are possible and turbulence truly competes with chemical reaction on all scales. Unfortunately, the fast turbulent flame leading to DDT might be suited in this regime of high turbulent intensities and distributed reaction zones, which numerical modelling must encounter. Since turbulent combustion itself generates chemical fluctuations, temperature fluctuations (i.e., hot spots) and fine scale acoustic disturbances, the model chosen should be probabilistic in nature. Consequently, the method of transported probability density function (PDF) recently developed by Pope becomes more promising due to its stochastic processes and suitability for high turbulent intensities.

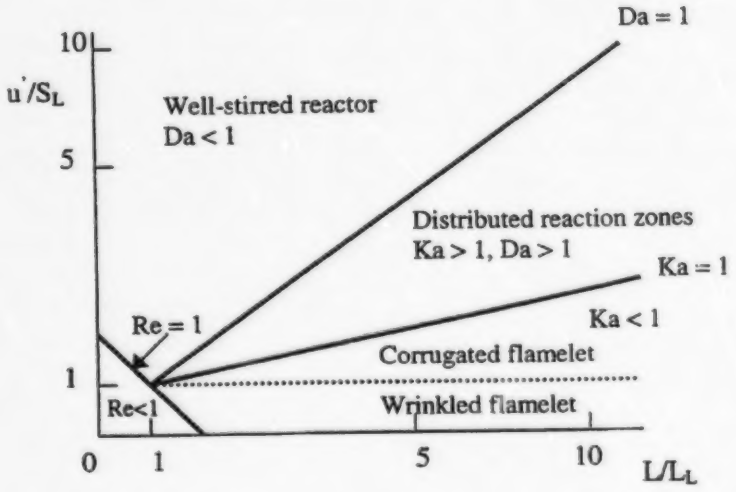

Figure 1. The Borghi diagram

Considering the FAE chemical initiation and the after-burning processes of oxygen-deficient explosives in various applications, DRES has been involved in investigations of different DDT mechanisms [7-8] and has sponsored Combustion Dynamics Ltd. in numerical modelling studies of this pioneer area [9-10]. This report was partially a result of these series of studies.

The objective of this work is a preliminary study in developing a numerical scheme that describes a quasi-one-dimensional turbulent flame structure associated with local points on the flame front in the distributed flame regime. This quasi-one-dimensional

model of flame structure can then be used in a front-tracking algorithm that simulates a DDT process triggered by a mild ignition [11]. Considering the objective, the theoretical model was based on the transported probability density function (PDF) method proposed by Pope [5, 12]. The primary advantage of the transported PDF method is that the effects of the reaction are in closed form. A hybrid scheme was developed in which the chemical compositions and enthalpy were computed using the PDF transport equations solved by the Monte Carlo method, while the mean flow field was solved by conventional finite volume techniques. Only the single-point, single-time joint scalar PDF transport equations were considered. Hybrid schemes can be found in the works including Pope et al. [21, 22, 24], Jones et al. [32, 34], and Hsu et al. [29, 38]. One of the main differences between these works is the mean flow solver that is coupled with the transported scalar PDF method. For the mean flow solver of the scheme developed, we chose an algorithm proposed by Issa and it is called PISO for Pressure-Implicit with Splitting of Operators [58-64]. The PISO algorithm is assumed to be capable for a large range of flow Mach numbers.

2. Monte Carlo method for scalar PDF transport equations

2.1. The joint scalar PDF equations for compressible flows

For quasi-one-dimensional compressible flows, the governing equations for the chemical compositions and enthalpy can be obtained from conservation principles:

$$\rho\frac{\partial Y_i}{\partial t}+\rho u\frac{\partial Y_i}{\partial x}=-\frac{\partial J_i}{\partial x}+\rho\dot{w},\quad i=1,\ldots,n$$
$$\rho\frac{\partial h}{\partial t}+\rho u\frac{\partial h}{\partial x}=-\frac{\partial J_q}{\partial x}+\frac{Dp}{Dt}+\tau_x\frac{\partial u}{\partial x}. \tag{2.1}$$

They can be written in a unified form:

$$\rho\frac{\partial \phi}{\partial t}+\rho u\frac{\partial \phi}{\partial x}=-\frac{\partial \mathbf{J}}{\partial x}+\rho\mathbf{S}, \tag{2.2}$$

where

$$\phi=\left[Y_1,\ldots,Y_n,h\right]^T,\ \mathbf{J}=\left[J_1,\ldots,J_n,J_q\right]^T,$$

$$\mathbf{S}=\left[\dot{w}_1,\ldots,\dot{w}_n,\frac{1}{\rho}\left(\frac{Dp}{Dt}+\tau_x\frac{\partial u}{\partial x}\right)\right]^T.$$

The joint scalar PDF of ϕ, $P(\psi;x,t)$ contains all single point, single time moments of the scalar field. ψ is the n+1 dimensional scalar space corresponding to ϕ, and a given

location in scalar space, $\Psi = \Psi'$, corresponds to fluid of properties $\Phi = \Psi'$. Following the methodology stated in [12, 36], the transport equation for $P(\psi; x, t)$ can be obtained from (2.2) and the continuity equation

$$\frac{\partial \rho}{\partial t} + \frac{\partial (\rho u)}{\partial x} = \rho S_\rho \tag{2.3}$$

where S_ρ is the source term for the effects of the flame front curvature. The equation for $P(\psi; x, t)$ is

$$\begin{aligned} \frac{\partial}{\partial t}(\rho P) + \frac{\partial}{\partial x}(\rho \tilde{U} P) + \sum_{\alpha=1}^{n} \frac{\partial}{\partial \psi_\alpha}(\rho S_\alpha P) &= -\frac{\partial}{\partial x}\left[\rho \langle u'' | \psi \rangle P\right] \\ + \sum_{\alpha=1}^{n+1} \frac{\partial}{\partial \psi_\alpha}\left[\left\langle \frac{\partial J_\alpha}{\partial x} \middle| \psi \right\rangle P\right] - \frac{\partial}{\partial \psi_{n+1}}\left[\rho \langle S_{n+1} | \psi \rangle P\right] &+ \rho \langle S_\rho | \psi \rangle P \end{aligned} \tag{2.4}$$

The terms in (2.4), from the left to right, represent:

- rate of change in physical space,
- mean convection in physical space,
- source production in compositional space,
- turbulent transport in physical space,
- molecular mixing in n+1 dimensional scalar space,
- source production due to compressibility,
- source production due to flame front curvature.

The terms on the left-hand side are in closed form provided $S_\alpha = S_\alpha(\phi)$, whereas the terms on the right-hand side contain conditional expectations that must be modeled.

—— Turbulent transport

The first term on the right-hand side represents transport in physical space due to turbulent velocity fluctuation. The scalar PDF $P(\psi; x, t)$ contains no information about velocities and the conditional expectation is then calculated using gradient-diffusion model [43]:

$$\overline{\rho} \langle u'' | \psi \rangle \rho P = -\Gamma_T \frac{\partial (\rho P)}{\partial x} \tag{2.5}$$

—— Molecular mixing

The second term on the right-hand side represents transport in n+1 scalar space due to molecular mixing. Several molecular mixing models have been proposed and reviews can

be found in [26, 30, and 57]. Coalescence-dispersion models are employed and they can be expressed in the general form [33]

$$\sum_{\alpha=1}^{n+1}\frac{\partial}{\partial\psi_\alpha}\left[\left\langle\frac{\partial J_\alpha}{\partial x}\middle|\psi\right\rangle P\right]=\overline{\rho}C_D\frac{\varepsilon}{k}\left[\int_\varphi d\varphi\int_\vartheta d\vartheta\tilde{P}(\varphi)\tilde{P}(\vartheta)T(\varphi,\vartheta|\psi)-\tilde{P}(\psi)\right] \tag{2.6}$$

Where $\tilde{P}$ is the density-weighted (Favre) joint PDF defined by

$$\tilde{P}=\rho P/\overline{\rho} \tag{2.7}$$

The function T is a transition PDF and in terms of Curl's model,

$$T(\varphi,\vartheta|\psi)=\delta\left[\psi-\tfrac{1}{2}(\varphi+\vartheta)\right] \tag{2.8}$$

—— Compressibility effect

The third term of the right-hand side represents the source production caused by the flow compressibility, where the conditional expectation is

$$\rho\left\langle S_{n+1}|\psi\right\rangle=\left\langle\frac{Dp}{Dt}\middle|\psi\right\rangle+\left\langle\tau_x\frac{\partial u}{\partial x}\middle|\psi\right\rangle \tag{2.9}$$

Appropriate modelling of these terms is important in understanding the role of the turbulence in fast flame regimes. Unfortunately, the dependence of the pressure and velocity fluctuations on the compositions and specific enthalpy are unknown. Even when one assumes that these fluctuations are statistically independent of the compositions and specific enthalpy, available models for the compressibility are limited (e. g., see [65]). Hsu et al. [29] simply neglects the energy dissipation term and proposed a model based on Sarkar's model for the pressure dilatation term and a second-order closure model for the trace of the pressure-strain rate. The model obtained is

$$\rho\left\langle S_{n+1}|\psi\right\rangle=\frac{\partial\overline{p}}{\partial t}+\tilde{U}\frac{\partial\overline{p}}{\partial x}+\alpha_1\overline{\rho}k\frac{\partial\tilde{U}}{\partial x}-\alpha_2\overline{\rho}\,\mathrm{Pr}\,M_t+\alpha_3\overline{\rho}\varepsilon M_t^2 \tag{2.10}$$

where $\alpha_1=0.8$, $\alpha_2=0.15$, $\alpha_3=0.2$.

—— Front curvature effect

Following Wood and Kirkwood [66], the effect of the front curvature is modeled using a cross-section area change in a duct:

$$S_\rho=-\kappa\tilde{U}=-\frac{1}{A}\frac{dA}{dx}\tilde{U} \tag{2.11}$$

Simply assuming that the curvature quantity is statistically independent of the compositions and specific enthalpy, one obtains

$$\rho\langle S_\rho|\psi\rangle P = -\kappa\rho\tilde{U}P \tag{2.12}$$

For the preliminary test of the scheme, a constant κ is further assumed in the flame structure:

$$\kappa = cH(\tilde{U} - \tilde{U}_{in}). \tag{2.13}$$

In (2.13), c is a constant, H is the heavy-side function and $\tilde{U}_{in}$ is the Favre-averaged flow velocity ahead of the flame front.

2.2. Monte Carlo method

The solution procedure for the scalar PDF equation (2.4) follows Pope's Monte-Carlo method [5, 12]. Equation (2.4) is discretized using an explicit forward time finite-difference scheme that is based on the technique of operator splitting:

$$\tilde{P}(\psi; x, t+\Delta t) = (\mathbf{I} + \mathbf{E}\Delta t)(\mathbf{I} + \mathbf{S}\Delta t)(\mathbf{I} + (\mathbf{C} + \mathbf{D})\Delta t)\tilde{P}(\psi; x, t) + \Delta t 0(\Delta x, \Delta t) \tag{2.14}$$

Here, **I** is the unit matrix, and **E**, **S**, **C** and **D** are difference coefficient matrices associated with the molecular mixing, the source production including chemical reactions and compressibility, convective transport and diffusion transport, respectively. The source production of flame curvature is included in the operator **C**. Equation (2.14) is fully explicit and first-order accurate. It can be solved in a sequence of operation:

$$\begin{aligned}
\tilde{P}(\psi; x, t+\Delta t') &= (\mathbf{I} + (\mathbf{C} + \mathbf{D})\Delta t)\tilde{P}(\psi; x, t) \\
\tilde{P}(\psi; x, t+\Delta t'') &= (\mathbf{I} + \mathbf{S}\Delta t)\tilde{P}(\psi; x, t+\Delta t') \\
\tilde{P}(\psi; x, t+\Delta t) &= (\mathbf{I} + \mathbf{E}\Delta t)\tilde{P}(\psi; x, t+\Delta t'')
\end{aligned}, \tag{2.15}$$

The Monte Carlo method is a statistic simulation of the finite difference approximation, equation (2.14), on a Cartesian grid. Rather than considering $\tilde{P}(\psi; x, t)$ explicitly, the dependent variables in the simulation are values of ϕ carried by an ensemble of N "representative" particles located in each grid cell:

$$\Phi(x_i,t)=\begin{bmatrix}\phi^{(1)}(x_i,t)\\ \bullet\\ \bullet\\ \phi^{(N)}(x_i,t)\end{bmatrix}=\begin{bmatrix}Y_1^{(1)} & \bullet & \bullet & Y_n^{(1)} & h^{(1)}\\ \bullet & & \bullet & \bullet & \bullet\\ \bullet & & \bullet & \bullet & \bullet\\ Y_1^{(N)} & \bullet & \bullet & Y_n^{(N)} & h^{(N)}\end{bmatrix}. \tag{2.16}$$

Here, x_i refers to the coordinates pertaining to the finite difference grid. The ensemble average of any function $Q(\phi)$ is then defined by

$$\langle Q(\phi(x_i,t))\rangle=\frac{1}{N}\sum_{q=1}^{N}Q\left(\phi^q(x_i,t)\right) \tag{2.17}$$

Pope [5] stated: if for all functions Q, the ensemble average $\langle Q\rangle$ converges in probability to the expected value $\tilde{Q}$, then $\Phi(x_i,t)$ and $\tilde{P}(\psi;x_i,t)$ are equivalent.

—— Transport of convection and diffusion

The process of transport of convection and diffusion in physical space is schematically illustrated in Fig. 2. Particles at cell x_i would interact with those at neighbor cells x_{i-1} and x_{i+1} by applying the transport operator to random sampling.

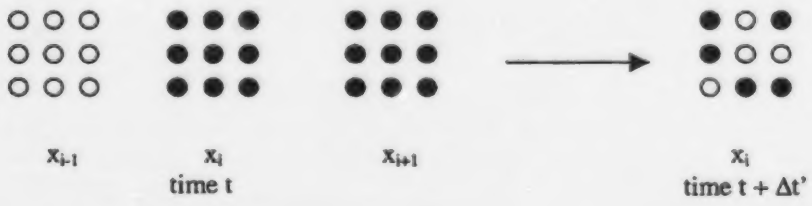

Figure 2. Schematic of the convection and diffusion transport of representative particles.

For the transport of diffusion, the new ensemble at cell x_i at time $t+\Delta t'$, $\Phi(x_i,t+\Delta t')$ contains Nx_{i-1} representative particles from $\Phi(x_{i-1},t)$, Nx_{i+1} representative particles from $\Phi(x_{i+1},t)$ and $N - Nx_{i-1} - Nx_{i+1}$ representative particles from $\Phi(x_i,t)$. The number of representative particles being transported ensures the equivalence between the Monte Calro simulation and the finite difference solution and they can be obtained by

$$Nx_{i\pm1}=N\frac{\Delta t}{\tau_{i\pm}^{d}} \tag{2.18}$$

with the diffusion time scale given by

$$\tau_{i\pm}^{d} = \frac{\overline{\rho}\Delta x^2}{\Gamma_T\left(x_i \pm \frac{1}{2}\Delta x, t\right)} > \Delta t \tag{2.19}$$

The representative particles being transported are selected at random using a random number generator with a uniform distribution in the interval [0, 1]. Note that the newly formed ensemble is not used during the randomly selecting loop, but the original ensemble illustrated on the left-hand side of the arrow in Fig. 2 is employed.

The transport of convection follows the same procedure described above. However, using upwind differencing, the new ensemble at cell x_i at time $t + \Delta t'$, $\Phi(x_i, t+\Delta t')$ contains $N - Nc_i$ representative particles from $\Phi(x_i, t)$ and Nc_i representative particles from $\Phi(x_{i-1}, t)$ or $\Phi(x_{i+1}, t)$, depending on the direction of the local velocity. The number of the representative particles being transported can be obtained by

$$Nc_i = N\frac{\Delta t}{\tau_i^c} \tag{2.20}$$

with the convection time scale given by

$$\tau_i^c = \frac{\Delta x}{\left|\tilde{U}_i(x_i, t)\right|} > \Delta t \tag{2.21}$$

—— Source production

The source production of chemical reactions and compressibility is performed in composition and specific enthalpy space. Consequently, this is simulated by changing the composition and specific enthalpy of each representative particle at each cell. A physical interpretation of the process is simply that each representative particle reacts independently for an interval of time Δt according to the ordinary differential equations:

$$\frac{d\phi^{(p)}}{dt} = S^{(p)}, \quad p \in [1, N] \tag{2.22}$$

Input of a reaction mechanism is required for evaluating the reaction rates, and the NASA polynomials are used to relate the specific enthalpy with the temperature. The ODE system (2.22) is then solved by VODE [67-68].

—— Molecular mixing

The molecular mixing takes place in composition and specific enthalpy space. Therefore, the process is simulated by randomly mixing compositions and enthalpies of

representative particles at each cell. The new ensemble at cell x_i at time t + Δt, $\Phi(x_i, t+\Delta t)$ contains N - $2Nm_i$ representative particles selected at random from $\Phi(x_i, t+\Delta t")$ and $2Nm_i$ representative particles being "mixed". The number of pairs of representative particles selected for mixing is

$$Nm_i = \frac{N}{2}\frac{\Delta t}{\tau_i^m} \tag{2.23}$$

with the mixing time scale given by

$$\tau_i^m = \frac{k_i}{C_d \varepsilon_i} > \Delta t \tag{2.24}$$

where C_d = 6. The representative particles being mixed are selected at random using a random number generator with a uniform distribution in the interval [0, 1].

In the present work, the Curl model and modified Curl model are implemented and they can be written as

$$\begin{aligned} \phi^{(p)}(x_i, t+\Delta t) &= a\phi^{(q)}(x_i, t+\Delta t") + (1-a)\phi^{(p)}(x_i, t+\Delta t") \\ \phi^{(q)}(x_i, t+\Delta t) &= a\phi^{(p)}(x_i, t+\Delta t") + (1-a)\phi^{(q)}(x_i, t+\Delta t") \end{aligned} \tag{2.25}$$

Where a = 0.5 is for the Curl model and a = 0.5 multiplied by a uniformly distributed random number in the interval [0, 1] for the modified Curl model.

3. PISO method for mean flow equations

3.1. The quasi-one-dimensional mean flow equations

For quasi-one-dimensional compressible flows, the governing transport equations for continuity, momentum, energy, turbulent kinetic energy and its rate of dissipation are:

$$\frac{\partial \rho}{\partial t} + \frac{\partial}{x^\alpha \partial x}\left(x^\alpha \rho \tilde{U}\right) = \rho S_\rho \tag{3.1}$$

$$\frac{\partial}{\partial t}\left(\rho \tilde{U}\right) + \frac{\partial}{x^\alpha \partial x}\left(x^\alpha \rho \tilde{U}^2\right) = -\frac{\partial p}{\partial x} + \frac{\partial}{x^\alpha \partial x}\left(x^\alpha \tau_{xx}\right) - \alpha\frac{\tau_{\theta\theta}}{x} + \rho S_M \tag{3.2}$$

$$\frac{\partial}{\partial t}(\rho e)+\frac{\partial}{x^{\alpha}\partial x}\left(x^{\alpha}\rho\tilde{U}e\right)=-\frac{\partial}{x^{\alpha}\partial x}\left(x^{\alpha}p\tilde{U}\right)+\frac{\partial}{x^{\alpha}\partial x}\left(x^{\alpha}\tau_{xx}\tilde{U}\right)+\frac{\partial}{x^{\alpha}\partial x}\left[x^{\alpha}\mu_{T}\frac{\partial h}{\partial x}\right]+\frac{\partial}{x^{\alpha}\partial x}\left[x^{\alpha}\mu_{k}\frac{\partial k}{\partial x}\right]+\rho S_{E} \tag{3.3}$$

$$\frac{\partial}{\partial t}(\rho k)+\frac{\partial}{x^{\alpha}\partial x}\left(x^{\alpha}\rho\tilde{U}k\right)=\frac{\partial}{x^{\alpha}\partial x}\left[x^{\alpha}\mu_{k}\frac{\partial k}{\partial x}\right]+P_{k}-(1+\xi M_{t}^{2})\rho\varepsilon+D+\rho S_{k} \tag{3.4}$$

$$\frac{\partial}{\partial t}(\rho\varepsilon)+\frac{\partial}{x^{\alpha}\partial x}\left(x^{\alpha}\rho\tilde{U}\varepsilon\right)=\frac{\partial}{x^{\alpha}\partial x}\left[x^{\alpha}\mu_{\varepsilon}\frac{\partial\varepsilon}{\partial x}\right]+[C_{1}f_{1}P_{k}-C_{2}f_{2}\rho\varepsilon]\frac{\varepsilon}{k}+E+\rho S_{\varepsilon} \tag{3.5}$$

Note that all the variables in this section are the mean flow variables and for simplicity the Reynolds-averaged mean value symbol is omitted. The variable e is the specific total energy:

$$e=e_{int}(T)+\tfrac{1}{2}\tilde{U}^{2}+k \tag{3.6}$$

The index $\alpha=0$ is for the planar case, $\alpha=1$ for the cylindrical symmetry and $\alpha=2$ for the spherical symmetry. The quasi-1D source terms are:

$$\begin{aligned} S_{M}&=S_{\rho}\tilde{U}\\ S_{E}&=S_{\rho}(e+p/\rho)\\ S_{k}&=S_{\rho}k\\ S_{\varepsilon}&=S_{\rho}\varepsilon \end{aligned} \tag{3.7}$$

where $S_{\rho}=0$ is for $\alpha>0$ and S_{ρ} is obtained from (2.11) and (2.13) when $\alpha=0$. For the quasi-1D compressible flows discussed, only the case of $\alpha=0$ will be considered.

The shear stresses can be obtained by

$$\begin{aligned} \tau_{xx}&=\mu_{E}\left(\frac{4}{3}\frac{\partial\tilde{U}}{\partial x}-\frac{2}{3}\alpha\frac{\tilde{U}}{x}\right)-\frac{2}{3}\rho k\\ \tau_{\theta\theta}&=\mu_{E}\left[-\frac{2}{3}\frac{\partial\tilde{U}}{\partial x}+2\left(1-\frac{\alpha}{3}\right)\frac{\tilde{U}}{x}\right]-\frac{2}{3}\rho k \end{aligned} \tag{3.8}$$

and the turbulent production by

$$P_{k}=2\mu_{t}\left[\left(\frac{\partial\tilde{U}}{\partial x}\right)^{2}+\alpha\left(\frac{\tilde{U}}{x}\right)^{2}\right]-\frac{2}{3}\left[\mu_{t}\frac{\partial}{x^{\alpha}\partial x}\left(x^{\alpha}\tilde{U}\right)+\rho k\right]\frac{\partial}{x^{\alpha}\partial x}\left(x^{\alpha}\tilde{U}\right). \tag{3.9}$$

The viscosities presented in the governing equations can be obtained by

$$\begin{aligned}
\mu_t &= f_\mu C_\mu \frac{\rho k^2}{\varepsilon} \\
\mu_E &= \mu_L + \mu_t \\
\mu_T &= \frac{\mu_L}{Pr_L} + \frac{\mu_t}{Pr_t} \\
\mu_k &= \mu_L + \frac{\mu_t}{Pr_k} \\
\mu_\varepsilon &= \mu_L + \frac{\mu_t}{Pr_\varepsilon}
\end{aligned} \qquad (3.10)$$

and the turbulence Mach number by

$$M_t^2 = 2k/a^2 . \qquad (3.11)$$

Note that the energy equation (3.3) is presented only for the completeness. When coupled with the joint scalar PDF equation (2.4), the energy equation (3.3) will not be used. Thus, the mean flow solution is obtained using equations (3.1), (3.2), (3.4), (3.5) and the equation of state:

$$\rho = p\sigma(p, T) \qquad (3.12)$$

For an ideal gas σ becomes $\overline{W}/(R_u T)$.

Table 1: Variables and functions in equation (3.13)

Φ	$\Gamma\frac{\partial\Phi}{\partial x}$	Q_Φ
$\tilde{U}$	$\frac{4}{3}\mu_E\frac{\partial\tilde{U}}{\partial x}$	$-\frac{\partial p}{\partial x}-\frac{2}{3}\frac{\partial}{x^\alpha\partial x}\left[x^\alpha\left(\alpha\mu_E\frac{\tilde{U}}{x}+\rho k\right)\right]-\alpha\frac{\tau_{\theta\theta}}{x}+\rho S_M$
e	$\mu_T\frac{\partial e}{\partial x}$	$-\frac{\partial}{x^\alpha\partial x}\left(x^\alpha p\tilde{U}\right)+\frac{\partial}{x^\alpha\partial x}\left(x^\alpha\tau_{xx}\tilde{U}\right)+\frac{\partial}{x^\alpha\partial x}\left[x^\alpha\mu_T\frac{\partial}{\partial x}\left(\frac{p}{\rho}\right)\right]$ $+\frac{\partial}{x^\alpha\partial x}\left[x^\alpha\mu_k\frac{\partial k}{\partial x}\right]+\rho S_E$
k	$\mu_k\frac{\partial k}{\partial x}$	$P_k-(1+\xi M_t^2)\rho\varepsilon+D+\rho S_k$
ε	$\mu_\varepsilon\frac{\partial\varepsilon}{\partial x}$	$[C_1 f_1 P_k - C_2 f_2\rho\varepsilon]\frac{\varepsilon}{k}+E+\rho S_\varepsilon$

The equations for momentum, energy, k and ε can be written in a unified form:

$$\frac{\partial}{\partial t}(\rho\Phi)+\frac{\partial}{x^{\alpha}\partial x}\left(x^{\alpha}\rho\tilde{U}\Phi\right)-\frac{\partial}{x^{\alpha}\partial x}\left(x^{\alpha}\Gamma\frac{\partial\Phi}{\partial x}\right)=Q_{\Phi} \tag{3.13}$$

with its variables and functions listed in table 1.

3.2. Modified PISO method

3.2.1. Discretization

The algorithm for the mean flow solution is based on the PISO scheme (Pressure-Implicit with Splitting of Operators) [58-60]. A staggered grid arrangement, depicted in Fig. 3, is employed in which velocity nodes are located in between those for scalar variables including pressure, energy, turbulent kinetic energy and its rate of dissipation. The spatial variations are approximated by upwind difference for convection and central difference for diffusion, giving second-order spatial accuracy. The temporal discretization uses first-order Euler implicit difference formula. TVD-type limiter constraints are employed to eliminate solution oscillations in high-speed flows [62-64].

The derivation of the difference equations can be illustrated by considering equation (3.13). Integration of (3.13) over a control volume shown in Fig. 3 (with a scalar control volume for energy, k and ε equations, and a velocity control volume for momentum equation) gives

$$\frac{\rho^{*}\Phi^{**}-(\rho\Phi)^{n}}{\Delta t}+\frac{F_{e}^{c}\left(\Phi^{**}\right)-F_{w}^{c}\left(\Phi^{**}\right)}{x^{\alpha}\Delta x}-\frac{F_{e}^{d}\left(\Phi^{**}\right)-F_{w}^{d}\left(\Phi^{**}\right)}{x^{\alpha}\Delta x}=\left(Q_{\Phi}\right)^{*} \tag{3.14}$$

Here, F^{c} is the discretized convective flux obtained from upwind difference with TVD-type limiter constraints, and F^{d} is the discretized diffusive flux obtained from central difference. Rearrangement of (3.14) provides

$$\left(\frac{\rho_{i}^{*}}{\Delta t}-A^{*}\right)\Phi_{i}^{**}=H^{*}\left(\Phi_{j\neq i}^{**}\right)+\frac{\rho_{i}^{n}}{\Delta t}\Phi_{i}^{n}+\left(Q_{\Phi}\right)^{*},\quad i=1,\ldots,m. \tag{3.15}$$

for $\Phi=e,\tilde{U},k,\text{and}\,\varepsilon$. In equation (3.15), m is the cell number in the x-direction, superscript "*" refers to the value of the previous iteration and superscript "**" refers to the value of the current iteration. Equation (3.15) forms a linear equation system with a tri-diagonal coefficient matrix.

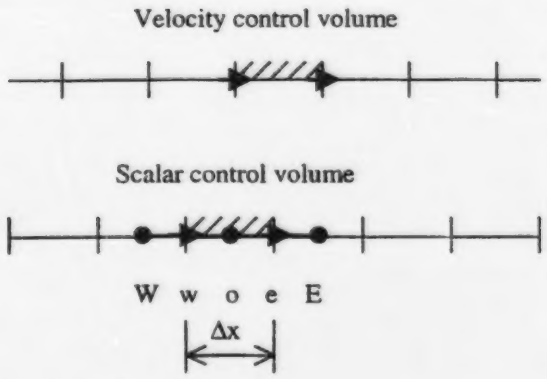

Figure 3. Control volumes for velocity and scalar variables.

An implicit equation for pressure is derived through combining the momentum and continuity equations. The obtained pressure equation is a linear equation system with a tri-diagonal coefficient matrix:

$$\Delta_i\left(\frac{x^\alpha}{a_p^*}\Delta_{i+1/2}\,p^{**}\right)-\frac{x^\alpha\sigma^*}{\Delta t}p^{**}=\Delta_i S^*-x^\alpha\rho^*\left(S_\rho\right)^*-\frac{x^\alpha\rho^n}{\Delta t} \tag{3.16}$$

where coefficients are

$$a_p^*=\frac{1}{\Delta t}-\frac{A^*}{x^\alpha\rho^*}, \tag{3.17}$$

$$S^*=\frac{1}{a_p^*}\left[H^*\left(\tilde{U}^*_{j\neq i}\right)-\frac{2}{3}\Delta_i\left[x^\alpha\left(\alpha\mu_E^*\frac{\tilde{U}^*}{x}+\rho^*k^*\right)\right]-\alpha x^{\alpha-1}\tau^*_{\theta\theta}+x^\alpha\rho^*\left(S_M\right)^*+\frac{x^\alpha\rho^n\tilde{U}^n}{\Delta t}\right]. \tag{3.18}$$

and the difference operator is

$$\Delta_i\Phi=\frac{\Phi_{i+1/2}-\Phi_{i-1/2}}{\Delta x} \tag{3.19}$$

In arriving at the pressure equation (3.16), the equation of state (3.12) has been invoked. The difference coefficient A* and H* are obtained from the discretization of the momentum equation (see (3.15)). Coefficients a_p and S are also derived from the momentum equation and are therefore stored on the centers of the velocity control volumes. The pressure equation is solved on the scalar control volumes. The density is then solved using equation of state (3.12):

$$\rho^{**} = p^{**}\sigma^{*} \tag{3.20}$$

Upon solving the pressure, the velocity can be explicitly obtained from the momentum equation

$$\tilde{U}_i^{**} = \left(-\frac{x_i^{\alpha}\Delta_i p^{**}}{a_{p,i}^{*}} + S_i^{*} \right) \Big/ \left(x_i^{\alpha}\rho_i^{**} \right) \tag{3.21}$$

which is discretized on the velocity control volumes.

3.2.2. Splitting Procedure

—— Predictor step

The flow variables prevailing at time t^n are used for the quantities marked with superscript "*" in equations (3.15 – 3.21).

Equation (3.15) is solved in the sequence of $e, \tilde{U}, k, \text{and}\, \varepsilon$ by one of the standard techniques such as the ADI method to yield $e^{**}, \tilde{U}^{**}, k^{**}, \text{and}\, \varepsilon^{**}$ fields. Note that the order of solution of these equations is of no consequence, as all coefficients are based on the old time level values. The temperature T^{**} is then calculated from equation (3.6).

Flow variables $e^{**}, \tilde{U}^{**}, k^{**}, \varepsilon^{**}$ and T^{**} are assigned to $e^{*}, \tilde{U}^{*}, k^{*}, \varepsilon^{*}$ and T^{*}.

—— Corrector step

Equations are solved in the following sequence.

1. Momentum corrector. Coefficients a_p^{*} and S^{*} are updated using equations (3.17 – 3.18). The pressure equation (3.16) is then solved using the ADI method to yield p^{**} field. Equation (3.20) yields ρ^{**} and equation (3.21) is explicitly solved to yield $\tilde{U}^{**}$ field. Variables p^{**}, ρ^{**}, and $\tilde{U}^{**}$ are assigned to p^{*}, ρ^{*}, and $\tilde{U}^{*}$.

2. k - ε corrector. The coefficients A^{*} and H^{*} in the k-equation (3.15) are updated to give the k-equation that is implicitly solved to yield k^{**} field. Similarly, the coefficient A^{*} and H^{*} in the ε-equation (3.15) are updated to give the ε-equation that yields ε^{**} field. Note that k-ε equations must be solved at the same level of iteration values, k^{*} and ε^{*}, to provide the solution stability. Variables k^{**} and ε^{**} are assigned to k^{*} and ε^{*}.

3. Energy corrector. The coefficient A^* and H^* in the energy equation (3.15) are updated to give the energy equation that is implicitly solved to yield e^{**} field. Equation (3.6) then gives temperature T^{**}. Variables e^{**} and T^{**} are assigned to e^* and T^*.

The corrector step is repeated until the convergence of solution is achieved. For problems tested, three times of corrector steps are usually sufficient to approach convergence. After the convergence, the density ρ^{**} is updated using equation (3.20) where σ^* is replaced by σ^{**}. The updated flow variables with superscript "**" are then taken to represent the field values at the next time level, n+1. This completes the sequence in the solution of the equations over the time step.

The original PISO scheme used variables Φ^* instead of Φ^{**} on the right hand side of equation (3.15) at corrector steps [58-60]. The equation (3.15) was therefore solved explicitly (a sort of semi-implicit scheme). However, that scheme required many times of the corrector step for convergence and often behaved unstable for turbulent flows particularly in the high-speed range or with reactions,. The implicit solution of equation (3.15) is more efficient than the semi-explicit solution with multiply corrector steps.

When coupled with the joint scalar PDF scheme, the solution steps for energy and temperature will be excluded in the predictor and corrector steps.

4. Coupling of Monte Carlo PDF and PISO mean flow scheme

The hybrid solution algorithm employed for turbulent flame structure computations involves the Monte-Carlo simulation to obtain the chemical compositions and temperature field, coupled with the modified PISO method for the density-weighted velocity, pressure, k and ε field. The latter field affects the former through the velocity, pressure, k and ε. In return, the Monte-Carlo method provides a mean density and temperature for use in solution of the mean flow. In the present work, the solution is limited to slow flows and the combustion is then assumed to take place at a constant pressure. The coupling of the Monte-Carlo simulation and the mean flow computation is sketched in Fig. 4. The algorithm is designed for unsteady flow problems and solution of a steady problem is treated as a time-asymptotic solution of an unsteady problem from its initial condition.

The time step of the hybrid algorithm is restricted to ensure the conditional stability of the explicit Monte-Carlo method depicted in equations (2.19), (2.21) and (2.24). These stability conditions are satisfied by the following criteria.

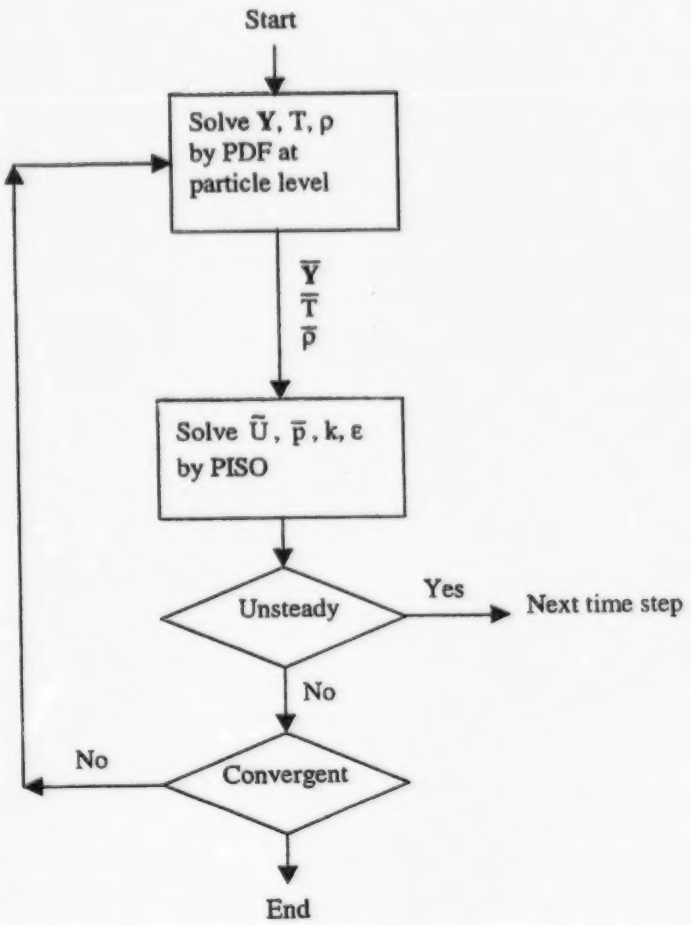

Figure 4. Coupling of the Monte Carlo pdf and PISO mean flow scheme.

—— Convection time step

$$\Delta t_c = \mathrm{cfl}\left(\min_i \frac{\Delta x}{|U_i(x_i,t)| + a_i} \right) \tag{4.1}$$

where cfl ≤ 1, a = 10 for subsonic flows and a is taken to be the local sound speed for supersonic flows.

—— Diffusion time step

For subsonic flows the diffusion time step is

$$\Delta t_d = \eta \left(\min_i \frac{\overline{\rho}_i \Delta x^2}{\Gamma_{Ti}} \right) \tag{4.2}$$

with

$$\Gamma_T = \frac{\mu_L}{Sc_L} + \frac{\mu_t}{Sc_t} \tag{4.3}$$

In equation (4.2), $\eta \leq 1/2$ and parameter Sc is the Schmidt number. $\Gamma_T = \mu_T$ when Sc = Pr. For supersonic flows, a simplified version of the criterion proposed by Kunz et al is used [69-70]:

$$\Delta t_d = \eta \left(\min_i \left[\frac{\upsilon_i}{\Delta x^2} + \Omega \right]^{-1} \right) \tag{4.4}$$

with

$$\upsilon_i = \frac{4\gamma\Gamma_{Ti} + 1/3\mu_{Ei}}{\overline{\rho}_i}, \tag{4.5}$$

$$\Omega = 2 \max \left(\frac{(P_k)_i}{\rho_i k_i}, \frac{C_2 f_2 \varepsilon_i}{k_i} \right). \tag{4.6}$$

The integration time step is then obtained by

$$\Delta t = \min(\Delta t_c, \Delta t_d) \tag{4.7}$$

5. An example: turbulent flame structure for a hydrogen-air mixture

Application of the quasi-1D PDF-module for the turbulent premixed flame structure is presented for a stoichiometric hydrogen-air mixture. The test cases include a planar turbulent flame structure without curvature source terms and that with curvature source terms. They are limited for the low Mach number flow and the last two source terms on the right hand side of equation (2.4) are not included yet. A six-step reduced hydrogen-air scheme is extracted from the detailed hydrogen reaction mechanism proposed by Maas and Warnatz [71], that is,

Chain Reactions :

$$O_2 + H \Leftrightarrow OH + O$$
$$H_2 + O \Leftrightarrow OH + H$$
$$H_2 + OH \Leftrightarrow H_2O + H$$
$$OH + OH \Leftrightarrow H_2O + O \qquad (4.8)$$

HO_2 Formation and Consumption :

$$O_2 + H + M \Leftrightarrow HO_2 + M$$
$$HO_2 + H \Leftrightarrow H_2 + O_2$$

The test cases are illustrated in Fig. 5 where a constant inflow boundary condition is used. An expanding grid ended by a zero-gradient outflow boundary is attached to the main grid of the flame structure computation. Usage of the expanding grid is to reasonably employ the grid resolution and to include the downstream flow influence on the flame structure.

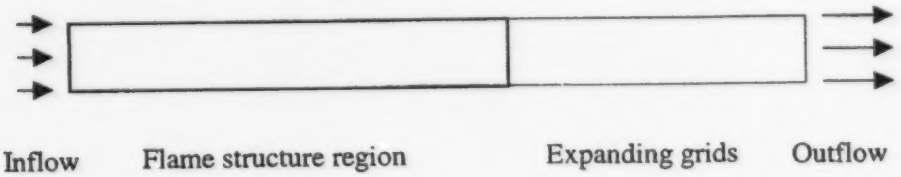

Figure 5. Test case for quasi-1D turbulent flame structure.

The propagation of the flame front is treated as a time-asymptotic solution of an unsteady problem from its initial condition. Initial conditions for the flow assume that, initially, the duct is entirely filled with the reactants at a high temperature which is less than and near the flame temperature. The initial velocity in the duct is uniform and equal to or greater than that of the low temperature gas to be injected. Alternatively, one can also fill the duct with the expected level of reaction products if they can be predicted. The pressure is taken to be constant along the length of the duct. When the duct is filled with the reactants initially, the flame front will travel downstream as the mixture undergoes ignition. A stationary flame can be obtained if the inlet flow velocity is equal to the flame velocity. The initial conditions for the test case without curvature source terms is listed in table 2. The flame structure region is 5 cm long and 10 cells are used for this region. The expanding grid has the same initial conditions as in the flame structure region and contains 5 cells with an expanding factor of 1.5. At any cell the PDF is simulated by 50 stochastic particles each of which carries the appropriate scalar properties. For the case including the effect of flame front curvature, the initial setup is the same, but with the

additional source terms, equations (2.11 and 3.7), depicted by a constant area change c = 50 m^{-1} in equation (2.13).

Table 2: Initial conditions for the test of turbulent premixed flame structure

Inflow:				
p, atm	T, K	u, m/s	k, J/kg	ε, J/kg-s
1	300	5	25	500
Y_H_2	Y_O_2	Y_N_2	Y_OH, Y_H_2O, Y_H, Y_O, Y_HO_2	
0.028521	0.226362	0.745117	0	
Flame structure region:				
p, atm	T, K	u, m/s	k, J/kg	ε, J/kg-s
1	1400	5	25	500
Y_H_2	Y_O_2	Y_N_2	Y_OH, Y_H_2O, Y_H, Y_O, Y_HO_2	
0.028521	0.226362	0.745117	0	

The computational results of the turbulent flame structure are displayed in Figs. 6 – 11 where the values of mean flow velocity, mean temperature, turbulent kinetic energy, its dissipation rate, and mean mass fractions of H_2, OH, O_2 and H_2O are plotted along the combustion zone. To learn the effects of the quasi-1D curvature source terms on the flame structure, comparison of the flame structure between with and without curvature source terms are provided in these figures.

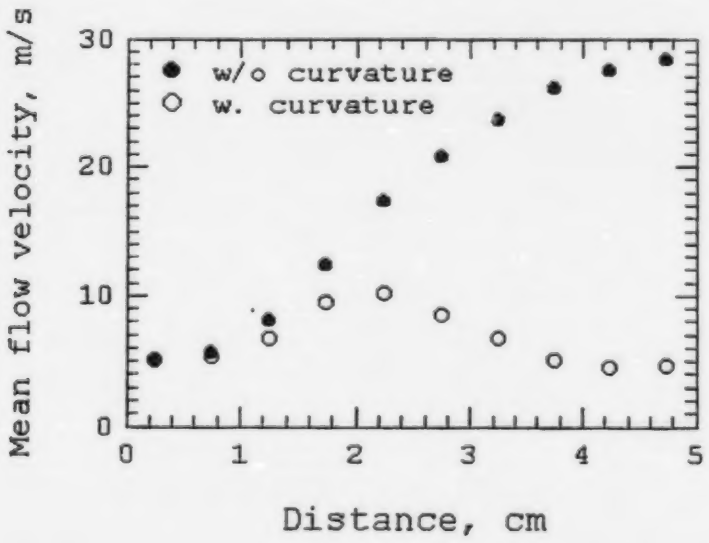

Figure 6. Mean flow velocity with and without curvature effects.

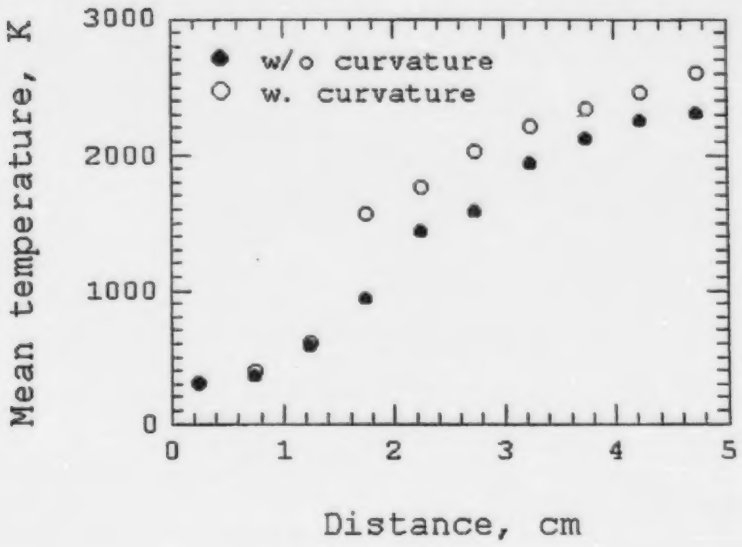

Figure 7. Mean temperature with and without curvature effects.

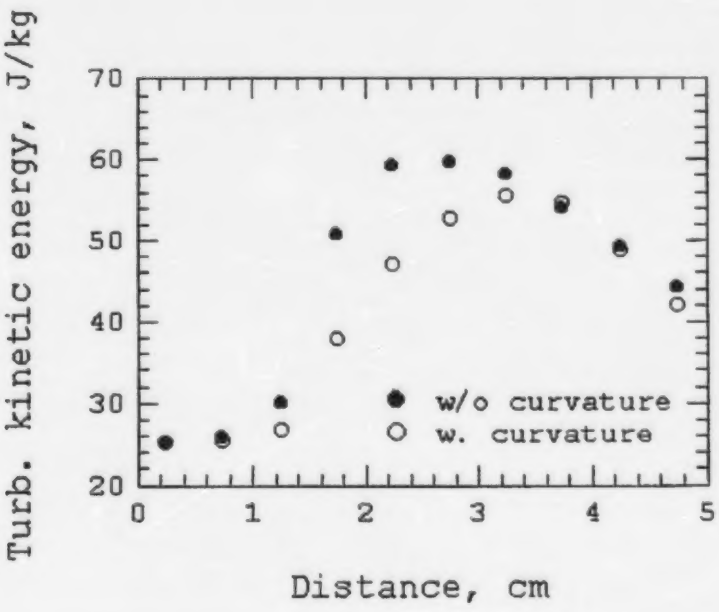

Figure 8. Turbulent kinetic energy with and without curvature effects.

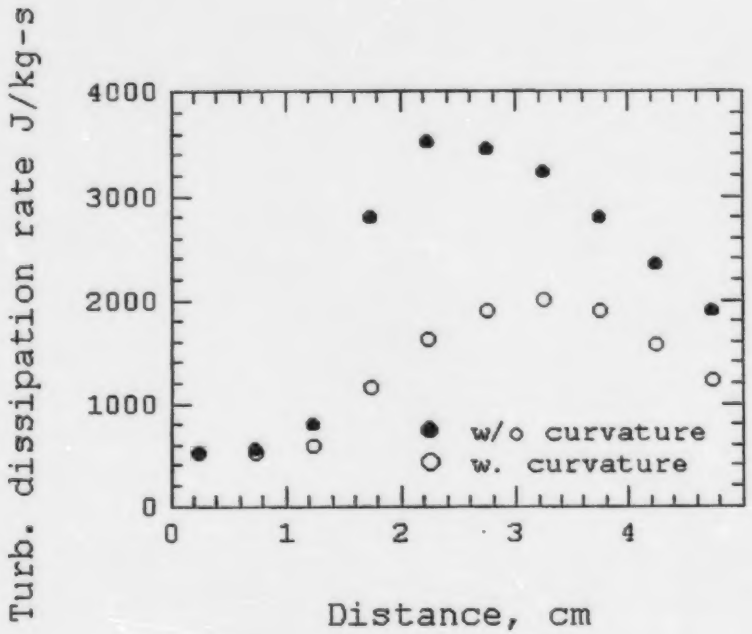

Figure 9. Turbulence dissipation rate with and without curvature effects.

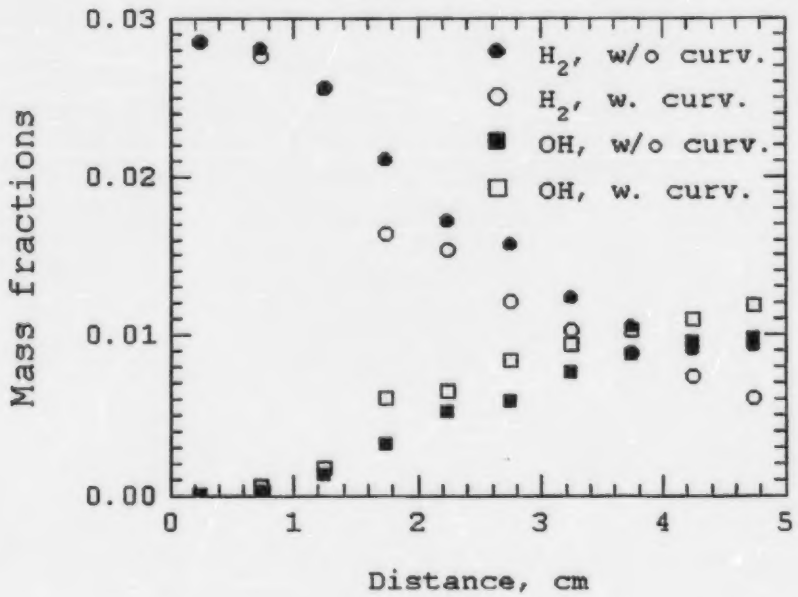

Figure 10. Mean mass fractions of H_2 and OH with and without curvature effects.

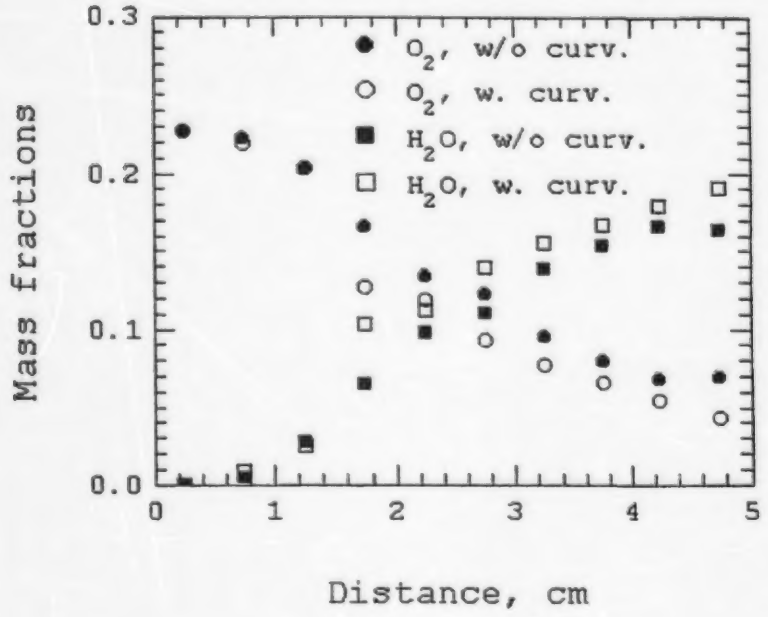

Figure 11. Mean mass fractions of O_2 and H_2O with and without curvature effects.

6. Conclusions

A quasi-1D PDF-module for the turbulent premixed flame structure was developed using a hybrid numerical scheme. In this scheme, the chemical compositions and enthalpy were computed using the Monte Carlo method for the joint scalar PDF transport equations where the single-point, single-time joint scalar PDF is considered only. The turbulent mean flow field was solved using a finite volume algorithm based on the PISO method for Pressure-Implicit with Splitting of Operators. The PISO algorithm was assumed to be capable for a range of flow Mach numbers. The effect of the flame front curvature was modeled by source terms that are analogous to a quasi-1D area change term. The code was implemented in an unsteady version and a quasi-steady solution for the turbulent flame structure was obtained as a time-asymptotic solution of an unsteady problem from its initial condition.

This work was focused on developing the numerical scheme that provides a platform for the further study of physical models. Thus, only basic models were used.

References

1. Murray, S.B. and Moen, I.O. (1987) Single-event fuel-air explosives: current Canadian and American Research (U). Defence Research Establishment Suffield Memorandum No. 1149 (CONFIDENTIAL)

2. Murray, S.B. (1998) Fuel-air and other low-density explosives: technology forecast to 2010 (U). Defence Research Establishment Suffield Memorandum No. 1514 (SECRET)

3. Bray, K.N.C., Libby, P.A. and Moss, J.B. (1985) Unified modeling approach for premixed turbulent combustion. Combustion and Flame 61:87-102

4. Peter, N. (1986) Laminar flamelet concepts in turbulent combustion. 21st Symp. (Intl.) on Combustion, The Combustion Institute, pp. 1231-1256

5. Pope, S. B. (1985) PDF methods for turbulent reactive flows. Prog. Energy Combust. Sci. 11:119-192

6. Libby, P.A. and Williams, F.A. (1994) Turbulent Reacting Flows. Academic Press, San Diego, CA

7. MacKay, D.J., Murray, S.B., Moen, I.O. and Thibault, P.A. (1988) Flame-jet ignition of large fuel-air clouds. Submitted to the 22nd Symposium (international) on Combustion, The Combustion Institute, Seattle, USA

8. Ritzel, D.V., Matthews, K., Hooton, L.E. and Murray, S.B. (1997) External Blast Ingress into Structures. The 15th International Symposium on Military Aspects of Blast and Shock, Bannf, Alberta, Canada

9. Numerical calculation of initiation of detonation in dispersed explosives. W7702-R7-2958 Final Report, Combustion Dynamics Ltd., 1995

10. Zhang, F. and Zhao, L. (1998) A PDF-module for turbulent flame structure computation. CDL Report.

11. Smiljanovski, V., Moser, V., and Klein, R. (1997) A cpapturing-tracking hybrid scheme for deflagration discontinuities. JCTM 1:183-215

12. Pope, S.B. (1981) A Monte Carlo method for the PDF equations of turbulent reactive flow. Combustion Science and Technology 25:159-174

13. Anand, M.S., Hsu, A.T. and Pope, S.B. (1996) PDF calculations for swirl combustors. AIAA-96-0522

14.Anand, M. S. and Pope, S. B. (1987) Calculation of premixed turbulent flames by pdf methods Combust. Flame 67:127-142

15.Chen, J-Y. (1988) Comb. Sci. Tech. 57:89.

16.Chen, H., Chen, S. and Kraichnan, R. H. (1989) Phys. Rev. Lett., 63:2657.

17.Chen, J-Y. and Dibble, R. W. (1990) In: Reduced Kinetic Mechanism and Asymptotic Approximations for Methane-Air Flames (M. D. Smooke Ed.)

18.Chen, J-Y. and Kollmann, W. (1990) Chemical models for pdf modeling of hydrogen-air non-premixed turbulent flames. Combst. Flame 79:75.

19.Chen, J-Y. and Kollmann W. (1990) 23rd Symp. (Intl.) on Combust., The Combustion Institute, Pittsburgh, PA, pp. 751-757.

20.Chen, J-Y., Kollmann, W. and Dibble, R. W. (1989) Comb. Sci. Tech. 64:315.

21.Chang, G. (1995) A Monto CarloPDF/Finite-Volume Study of Turbulent Flames. Ph.D. Thesis, Cornell University

22.Correa, S. M. and Braaten, M. E. (1993) Combust. Flame 94:469-486

23.Correa, S. M., Gulati, A. and Pope, S. B. (1994) Raman measurements and joint pdf modelling of a nonpremixed bluff-body-stabilized methane flame. 25th Symp. (Intl.) on Combustion, The Combustion Institute, Pittsburgh, PA, pp. 1167-1173

24.Correa, S. M. and Pope, S. B. (1992) Comparison of a Monte Carlo pdf/finite-volume mean flow model with bluff-body Raman data. 24th Symp. (intl.) on Combustion, Pittsburgh, PA, The Combustion Institute, pp. 279-285

25.Correa, S. M. and Shyy, W. (1987) Prog. Energy Comb. Sci. 13:249

26.Dopazo, C. (1994) Recent developments in PDF methods. In: Turbulent Reacting Flows, Libby, P.A. and Williams, F.A. (Eds), Academic Press

27. Dopazo, C. (1979) Relaxation of initial probablity density functions in the turbulent convention scalar fields. Physics of Fluids 22:20-30

28.Farshchi, M. (1989) A pdf closure model for compressible turbulent chemically reacting flow. AIAA-89-0390

29.Hsu, A.T., Tsai, Y.-L.P. and Raju, M.S. (1994) Probability density function approach for compressible turbulent reacting flows. AIAA J. 32:1407-1415

30.Jayesh and Pope, S.B (1995) Stochastic model for turbulent frequency. FDA 95-05, Cornell University

31.Janicka, J., Kobe, W. and Kollmann, W. (1979) Closure of the equations for the probability density function of turbulent scalar fields. Journal of non-Equilibrium Thermodynamics 4:47-66

32.Jones, W. P. (1994) The transported pdf approach to turbulent flames. Lecture Notes: Turbulent Combustion and its Modelling, ERCOFTAC Summer-school, University of Cambridge, September

33.Jones, W. P. and Kollmann, W. (1987) Multi-scalar transport equations for turbulent diffusion flames. In: Turbulent Shear Flows 5: Selected Papers. Springer-Verlag, pp. 269-309

34.Jones, W.P. and Prasetyo Y. (1996) Probablity density function modelling of premixed turbulent opposed jet flames. 26th Symp. (Intl.) on Combustion, The Combustion Institute

35.Kraichnan, R. H. (1990) Phys. Rev. Lett. 65:575

36.Kollmann, W. (1990) The pdf approach to turbulent flow. Theoretical and Computational Fluid Dynamics 1:249-285

37.Kollmann, W. (1992) Modelling of combustion and turbulence: pdf transport equation modelling. Von Karman Institute lecture series

38.Leonard, A.D. and Dai, F. (1994) Applications of a coupled Monte Carlo pdf/finite volume CFD method for turbulent combustion. AIAA-94-2904

39.Masri, A. R. and Pope, S. B. (1990) Combust. Flame 81:13

40.Maas, U. and Pope, S. B. (1992) Simplified chemical kinetics: intrinsic low-dimensional manifolds in composition space. Combust. Flame 88:239-264

41.Mass, U. and Pope, S. B. (1992) Implementation of simplified chemical kinetics based on intrinsic low-dimensional manifolds. 25th Symp. (Intl.) on Combustion, The Combustion Institute, pp. 103-112

42.Norris, A. T. and Pope, S. B. (1995) Modeling of extinction in turbulent diffusion flames by the velocity-dissipation-composition pdf method. Combust. Flame 100:211-220

43.Pope, S. B. (1976) Combust. Flame 27:299

44.Pope, S. B. (1982) An improved mixing model. Combustion Science and Technology 28:131-135

45.Pope, S. B. (1987) Turbulent premixed flames. Ann. Rev. Fluid Mech. 19:237-270.

46.Pope, S. B. (1990) Computations of turbulent combustion: progress and challenges. 23rd Symp. (Intl.) on Combustion, pp. 591-612

47.Pope, S. B. (1993) PDF/Monte Carlo methods for turbulent combustion and their implementation on parallel computers. In: Turbulent and Molecular Processes in Combustion (T. Takeno Ed.), pp. 51-62

48.Pope, S.B. (1993) On the relationship between stochastic Larangian models of turbulence and second-moment closures. Phys. Fluids 6:973-985

49.Pope, S. B. (1994) On the relationship between stochastic Lagrangian models of turbulence and second-moment closures. Phys. Fluids 6:973-985

50.Pope, S. B. (1994) Lagrangian pdf methods for turbulent flows. Annu. Rev. Fluid Mech. 26:23-63

51.Pope, S.B. (1995) Position, velocity and pressure correction algorithm for particle method solution of the pdf transport equations. FDA 95-06, Cornell University

52.Pope, S. B. and Anand, M. S. (1985) 20th Symp. (Intl.) on Combust., The Combustion Institute, Pittsburgh, PA, pp. 403.

53.Pope, S. B. and Cheng, W. K. (1988) 21st Symp. (intl.) on Combust., The Combustion Institute, Pittsburgh, PA, pp. 1473.

54.Ripley, B.D. (1987) Stochastic Simulation. J. Wiley, New York.

55.Smith, N. S. A., Bilger, R. W., and Chen, J-Y. (1992) 24th Symp. (Intl.) on Combustion, PA, pp. 263-269

56.Valino, L. and Dopazo, C (1991) A binomial Langevin model for turbulent mixing. Phys Fluids A 3:3034-3037

57.Subramaniam, S. and Pope, S. B. (1998) A mixing model for turbulent reactive flows based on Euclidean minimum spanning trees. Combust. Flame 115:487-514

58.Issa, R.I. (1985) Solution of the implicitly discretised fluid flow equations by operator-splitting. J. Comp. Phys. 62:40-65

59.Issa, R.I., Gosman, A.D. and Watkins, A.P. (1986) The computation of compressible and incompressible recirculating flows by a non-iterative implicit scheme. J. Comp. Phys.62:66-82

60.Issa, R.I., Ahmadi-Befrui, B., Beshay, K.R. and Gosman, A.D. (1991) Solution of the implicitly discretised reacting flow equations by operator-splitting. J. Comp. Phys. 93:388-410

61.Cant, R.S. and Bray, K.N.C. (1988) Stained laminar flamelet calculations of premixed turbulent combustion in a closed vessel. 22nd Symp. (Intl.) on Combustion, The Combustion Institute, pp. 791-799

62.Leonard, B.P. and Mokhtari S. (1990) Beyond first-order unwinding: the ultra-sharp alternative for non-oscillationary steady-state simulation of convection. International Journal for Numerical Methods in Engineering 30:729-766

63.Leonard, B.P. and Niknafs, H.S. (1991) Sharp monotonic resolution of discontinuities without clipping of narrow extrema. Computers & Fluids 19:141-154

64.Zhang, J., Tran, D. and Thibault, P. (1996) A study of numerical methods for a non-iterative implicit scheme at all Mach numbers. Proceedings of CFD96, CFD Society of Canada, pp. 59-66

65.Vandromme, D., Lebret, Y. and Dou, G. (1996) Supersonic turbulent modelling. In: Experimentation, modelling and computation in flow, turbulence and combustion, Desideri, J.A. and Chetverushkin, B.N., Kuznetsov, Y.A., Periaux, J. and Stoufflet, B. (eds), John Wiley & Sons, 183-201

66.Wood, W. W. and Kirkwood, J. G. (1954) Diameter effect in condensed explosives: the relation between velocity and radius of curvature in the detonation wave. J. Chem. Phys. 22:1920-1924

67.Byrne, G.D. (1992) The solution of a co-polymerization model with VODE. In: Recent Developments in Numerical Methods for ODEs/DAEs/PDEs, Byrne, G.D. and Schisser (eds), World Scientific, NJ, pp. 137-197

68.Brown, P.N., Bryne, G.D. and Hindmarch, A.C. (1989) VODE: a variable-coefficient ODE solver. SIAM J. Sci. Stat. Comput. 1038-1051

69.Kunz R.F. and Lakshminarayana, B. (1992) Explicit Navier-Stokes computation of Cascade flows using the k-ε turbulent model. AIAA J. 30:12-22

70.Kunz, R.F. and Lakshminarayana, B. (1992) Stability of explicit Navier-Stokes procedures using k-ε and algebraic Reynolds stress turbulence models. J. Comp. Phys. 103:141-159

71.Maas, U. and Warnatz, J. (1988) Ignition processes in hydrogen-oxygen mixtures. Combust. Flame 74: 53-69

UNCALSSIFIED
SECURITY CLASSIFICATION OF FORM
(highest classification of Title, Abstract, Keywords)

DOCUMENT CONTROL DATA

(Security classification of title, body of abstract and indexing annotation must be entered when the overall document is classified)

1. ORIGINATOR (the name and address of the organization preparing the document. Organizations for who the document was prepared, e.g. Establishment sponsoring a contractor's report, or tasking agency, are entered in Section 8.)

Defence Research Establishment Suffield
Box 4000 Medicine Hat, Alberta T1A 8K6

2. SECURITY CLASSIFICATION
(overall security classification of the document, including special warning terms if applicable)

UNCLASSIFIED

3. TITLE (the complete document title as indicated on the title page. Its classification should be indicated by the appropriate abbreviation (S, C or U) in parentheses after the title).

A PDF-MODULE FOR TURBULENT DEFLAGRATION STRUCTURE COMPUTATION

4. AUTHORS (Last name, first name, middle initial. If military, show rank, e.g. Doe, Maj. John E.)

Zhang, Fan

5. DATE OF PUBLICATION (month and year of publication of document)

November 1999

6a. NO. OF PAGES (total containing information, include Annexes, Appendices, etc) 28

6b. NO. OF REFS (total cited in document) 71

7. DESCRIPTIVE NOTES (the category of the document, e.g. technical report, technical note or memorandum. If appropriate, enter the type of report, e.g. interim, progress, summary, annual or final. Give the inclusive dates when a specific reporting period is covered.)

DRES Technical Report

8. SPONSORING ACTIVITY (the name of the department project office or laboratory sponsoring the research and development. Include the address.)

9a. PROJECT OR GRANT NO. (If appropriate, the applicable research and development project or grant number under which the document was written. Please specify whether project or grant.) N/A

9b. CONTRACT NO. (If appropriate, the applicable number under which the document was written.) N/A

10a. ORIGINATOR'S DOCUMENT NUMBER (the official document number by which the document is identified by the originating activity. This number must be unique to this document.)

DRES Technical Report TR 1999-020

10b. OTHER DOCUMENT NOs. (Any other numbers which may be assigned this document either by the originator or by the sponsor.)

N/A

11. DOCUMENT AVAILABILITY (any limitations on further dissemination of the document, other than those imposed by security classification)

- (x) Unlimited distribution
- ( ) Distribution limited to defence departments and defence contractors; further distribution only as approved
- ( ) Distribution limited to defence departments and Canadian defence contractors; further distribution only as approved
- ( ) Distribution limited to government departments and agencies; further distribution only as approved
- ( ) Distribution limited to defence departments; further distribution only as approved
- ( ) Other (please specify):

12. DOCUMENT ANNOUNCEMENT (any limitation to the bibliographic announcement of this document. This will normally corresponded to the Document Availability (11). However, where further distribution (beyond the audience specified in 11) is possible, a wider announcement audience may be selected).

Unlimited

ABSTRACT (a brief and factual summary of the document. It may also appear elsewhere in the body of the document itself. It is highly desirable that the abstract of classified documents be unclassified. Each paragraph of the abstract shall begin with an indication of the security classification of the information in the paragraph (unless the document itself is unclassified) represented as (S), (C) or (U). It is not necessary to include here abstracts in both official languages unless the text is bilingual).

In the FAE chemical initiation and the after-burning processes of oxygen-deficient explosives in various applications, a compressible, turbulent, fast me with a "thick" distributed reaction zone is encountered. Owing to the complicated interaction between turbulent mixing and combustion, the physical echanism for this fast turbulent flame regime leading to DDT has not been resolved and the numerical modelling is still in its pioneer stage.

This work was only a preliminary study in developing a model and its numerical scheme that describes a quasi-one-dimensional turbulent defraglation ucture associated with local points on the flame front in the distributed flame regime. This quasi-one-dimensional model of turbulent flame structure can in ure be coupled in a front-tracking algorithm that simulates the unsteady fast turbulent defraglation leading to a DDT process.

Owing to the stochastic nature and high turbulent intensity of the distributed flame regime, the model was based on Pope's PDF module and used a brid numerical scheme. In this scheme, the real chemical compositions and enthalpy were computed using the Monte Carlo method for the joint scalar DF transport equations to capture the stochastic non-uniformity of the chemical compositions and temperature. The turbulent mean flow field was solved ing a finite volume algorithm based on the method for pressure-implicit with splitting of operators to be compatible for a range of flow Mach numbers. The ect of the flame front curvature was modelled by source terms that are analogous to a quasi-1D area change term. The model was implemented in an steady version.

KEYWORDS, DESCRIPTORS or IDENTIFIERS (technically meaningful terms or short phrases that characterize a document and could be helpful in cataloguing the document. They should be selected so that no security classification is required. Identifies, such as equipment model designation, trade name, military project code name, geographic location may also be included. If possible keywords should be selected from a published thesaurus, e.g. Thesaurus of Engineering and Scientific Terms (TEST) and that thesaurus-identified. If it is not possible to select indexing terms which are Unclassified, the classification of each should be indicated as with the title.)

AE
DT
EFLAGRATION
IRBULENT COMBUSTION
DF
SO